Evaluation of edge effect due to phase contrast imaging for mammography

Satoru Matsuo[a)]
Department of Radiology, Shiga University of Medical Science, Shiga, Japan

Tetsuro Katafuchi
Department of Radiology, National Cardiovascular Center, Suita, Osaka, Japan

Keiko Tohyama
Kyoto College of Medical Technology, Kyoto, Japan

Junji Morishita
Department of Health Sciences, School of Medicine, Kyushu University, Japan

Katsuhiko Yamada
Kyoto College of Medical Technology, Kyoto, Japan

Hiroshi Fujita
Department of Intelligent Image Information, Graduate School of Medicine, Gifu University, Japan

(Received 25 July 2004; revised 6 June 2005; accepted for publication 10 June 2005; published 29 July 2005)

It is well-known that the edge effect produced by phase contrast imaging results in the edge enhancement of x-ray images and thereby sharpens those images. It has recently been reported that phase contrast imaging using practical x-ray tubes with small focal spots has improved image sharpness as observed in the phase contrast imaging with x-ray from synchrotron radiation or micro-focus x-ray tubes. In this study, we conducted the phase contrast imaging of a plastic fiber and plant seeds using a customized mammography equipment with a 0.1 mm focal spot, and the improvement of image sharpness was evaluated in terms of spatial frequency response of the images. We observed that the image contrast of the plastic fiber was increased by edge enhancement, and, as predicted elsewhere, spectral analysis revealed that as the spatial frequencies of the x-ray images increased, so did the sharpness gained through phase contrast imaging. Thus, phase contrast imaging using a practical molybdenum anode tube with a 0.1 mm-focal spot would benefit mammography, in which the morphological detectability of small species such as microcalcifications is of great concern. And detectability of tumor-surrounded glandular tissues in dense breast would be also improved by the phase contrast imaging. [DOI: 10.1118/1.1992087]

Key words: phase contrast imaging, edge enhancement, sharpness, mammography

I. INTRODUCTION

An x-ray is an electromagnetic wave, so that refraction and interference take place as generally observed with visible light. However, the refraction and the interference of x-rays have received little discussion because x-ray images have been depicted solely through the variation of image density (absorption contrast) resultant from the absorption of x-ray energy due to photoelectric effects and Compton scattering in objects. The phase shifting of electromagnetic waves takes place along with photoelectric effects and Compton scattering when x rays pass through objects. The phase shift is the origin of refraction and interference, and interference is limited when the x ray is highly coherent laterally. Somenkov and co-workers have reported that this phase shift can be imaged through refraction as phase contrast in x-ray imaging and that the sharpness of an x-ray image is improved by the concomitant edge enhancement of the x-ray images.[1] Depiction of x-ray images with phase contrast, in addition to absorption contrast, is the most highly efficient utilization of x-ray characteristics in x-ray imaging.[2]

In current medical radiography, images are created only via absorption contrast and not with phase contrast. This is because the deviation of refracted x-ray flux is as small as $10^{-6}-10^{-7}$ rad,[3] and because laterally coherent x-ray beams can be obtained from x-ray sources virtually as small as a point source, such as with micro-focus x-ray tubes for nondestructive inspection.[4] Recently Ohara and co-workers have reported on phase contrast imaging using a practical molybdenum anode tube with a 0.1 mm focal spot based upon incoherent x rays.[5] Freedman and co-workers have simulated improvement of image quality[6] with an analytical method which has been applied to phase contrast imaging using a tungsten anode x-ray tube.[7] In this study, we empirically evaluated and analyzed edge enhancement due to phase contrast in images of a plastic fiber and plant seeds. Our results indicate that phase contrast imaging promises benefits in application to mammography.

II. THEORY

In phase contrast imaging, two methods may be utilized: (1) Phase contrast extracted for imaging, and (2) phase con-

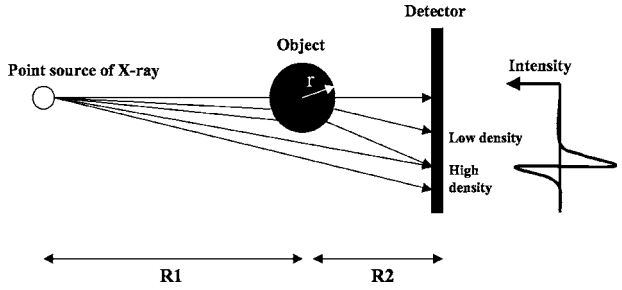

FIG. 1. Illustration of phase contrast imaging and edge effect with an x-ray point source. On the edge of the cylinder image, edge enhancement takes place due to refraction of the x-ray that is defined as phase contrast. The edge enhancement is shown schematically on the right side of the cylinder image in this figure.

trast superimposed on absorption contrast images.[8] In the former, monochromatic x-ray flux from synchrotron radiation is conjoined with Bragg refraction[9] or with an x-ray interferometer. In the latter,[10] x-ray imaging is conducted either with parallel monochromatic x-ray beams from synchrotron radiation[11]or polychromatic x-ray beams from point source x-ray tubes.[12] As shown in Fig. 1 with a micro-focus x-ray tube, x-ray flux increases just outside the edge of the cylindrical object image, and it decreases just inside the edge of the image, resulting in edge enhancement, or edge effect. Note that x-ray beams refract in the opposite direction of visible light. In this case of an ideal point x-ray source, blurring on the image plane is absent or negligible in the phase contrast imaging when an x-ray detector is placed some distance from the object; in the case of a practical medical x-ray tube, blurring is inevitable because of geometrical unsharpness.[13] When blurring threatens to obscure edge enhancement, geometric conditions must be dealt with.[14]

Ishisaka and co-workers have formulated the half width of edge enhancement, E, as defined in Fig. 2, assuming that the x-ray source is an ideal point source.[15]

$$E = 2.3(1 + R2/R1)^{1/3}\{R2\,\delta(2r)^{1/2}\}^{2/3}. \quad (1)$$

Note that $R1$ is the distance between the x-ray source and the center of an object, $R2$ is the distance between the center of the object and the image plane, r is radius of the cylindrical object, and the x-ray refractive index of solids is expressed as $n=1-\delta-i\beta$, where δ is the phase shift term, i is the square root of -1, and the β is the absorption term. An outline formulating the half width of the edge enhancement, E, is described in the Appendix.

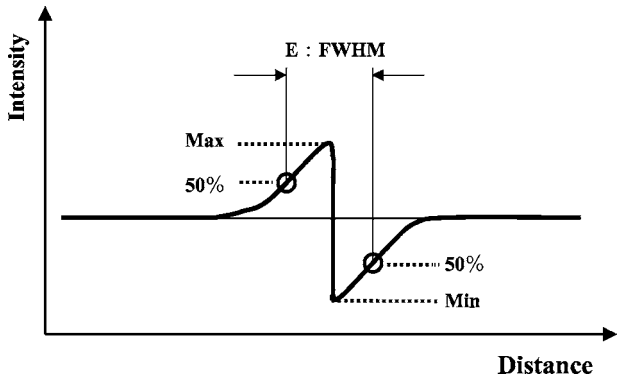

FIG. 2. Definition of full width at half maximum in edge enhancement due to phase contrast imaging.

Utilizing a practical x-ray tube with medical imaging, the x-ray detector such as a screen-film cassette is placed some distance from the object as in Fig. 1 for the phase contrast imaging, and this produces blurring on the x-ray detector due to the penumbra caused by the finite size of the focal spot, D. The width of the blurring, B, is calculated as below.

$$B = D(R2/R1). \quad (2)$$

It has been reported that blurring obliterates phase contrast when an x-ray tube with a focal spot size of 0.1 mm is employed in the geometry typical of medical imaging.[16] Nevertheless, phase contrast is still observed when the edge effect is sufficiently great in comparison to the blurring. Expressed another way, when Eq. (3) is satisfied, phase contrast is obtained even with practical medical x-ray tubes.

$$\kappa E \geqq B. \quad (3)$$

Note that κ is a positive constant which can be obtained empirically. When κ is small, a strong edge effect is necessary to detect the edge enhancement in the blurring in x-ray images, and vice versa. In the case of a molybdenum tube with a 0.1 mm focal spot, it has been simulated that phase contrast is obtained when κ is 9 or more.[14] Honda and coworkers have reported that simulations using Eqs. (1)–(3) for mammography with a 0.1 mm focal spot molybdenum tube have obtained edge enhancement from phase contrast when geometrical conditions were $R1 \geqq 0.5$ m and $R2 \geqq 0.25$ m.[15] Note that the longer the $R1$ is, the smaller the blurring is, and that the longer the $R2$ is, the greater is the diverge of refracted x-ray beams. The theory described above is applicable to phase contrast imaging with incoherent x-rays where the blurring on the image plane obscures interference of x-ray beams as described by Ishisaka and co-workers.[15]

III. MATERIALS AND METHODS

A. X-ray imaging

Customized x-ray mammography equipment (MGU-100B, Toshiba Medical Manufacturing Co., Ltd., Tokyo, Japan) was used to obtain the phase contrast imaging by use of longer source-to-object ($R1$) and object-to-image ($R2$) distances than normally used in mammography. The equipment included a molybdenum rotating anode tube with a 0.1 mm nominal focal spot.[6] Tube voltage was set to 26 kVp or 28 kVp depending on the object imaged (Table I). The geometrical conditions used for the phase contrast imaging, conventional contact imaging, and conventional 1.5× magnification imaging are shown in Fig. 3 and Table I. In no case was an anti-scattering x-ray grid used.

The x-ray detector used was a screen-film system consisting of a mammographic intensifying screen (MD-100, Konica-Minolta Medical and Graphic, Inc., Tokyo, Japan) and a mammographic film (New-CMH, Konica-Minolta

TABLE I. Imaging conditions used in this study.

Plastic fiber	kVp	mAs	R1 (cm)	R2 (cm)
Phase contrast imaging	26	10.0	100	50
Conventional 1.5 magnification	26	2.0	40	20
Conventional contact imaging	26	4.4	100	0
Seeds	kVp	mAs	R1 (cm)	R2 (cm)
Phase contrast imaging	28	17.0	100	50
Conventional 1.5 magnification	28	3.0	40	20
Conventional contact imaging	28	6.8	100	0

Medical and Graphic, Inc., Tokyo, Japan). Exposure conditions were adjusted to obtain 1.40±0.05 optical density. The exposed films were developed with an automatic processor (SRX-502, Konica-Minolta Medical and Graphic, Inc., Tokyo, Japan) with a 90 s cycle-time using processing chemicals, XD-SR for the developer at 35 °C and XF-SR for the fixer (Konica-Minolta Medical and Graphic, Inc., Tokyo, Japan). The obtained images of x-ray films were digitized with a sampling pitch of 0.025 mm using a drum-scan densitometer (Model 2605, Abe Sekkei, Tokyo, Japan). Digitized image data of the films were transformed into x-ray intensities by use of a measured digital characteristic curve. The consequent experimental procedures are shown in Fig. 4.

B. Measurement of image contrast

Using Eq. (4) below, we obtained the image contrast in the obtained x-ray intensity profiles for a plastic fiber with a 3 mm diameter. The definitions of *I* max and *I* min are given in Fig. 5. Phase contrast imaging was 1.5× magnification so that conventional contact imaging data could be extrapolated with a three-dimensional (3D) spline function allowing comparison of the same size.

$$\text{Contrast} = (I\,\text{max} - I\,\text{min})/((I\,\text{max} + I\,\text{min})/2). \quad (4)$$

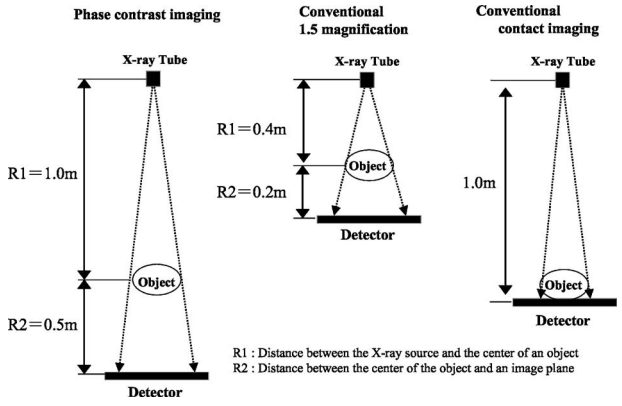

FIG. 3. Geometrical conditions for phase contrast imaging (left), conventional contact imaging (right), and conventional 1.5× magnification imaging (center). Note that the phase contrast imaging is also 1.5× magnification but whose the R1 and the R2 are longer than those for conventional 1.5× magnification imaging.

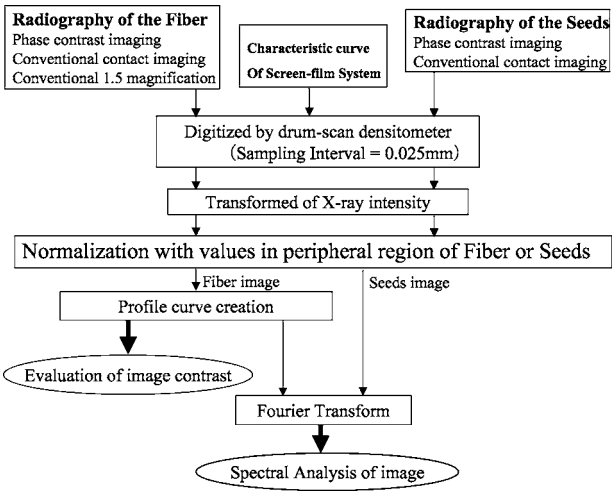

FIG. 4. A schematic diagram for procedure of spectral analysis of image quality for x-ray images. Test objects used in this study were plastic fiber and plant seeds.

C. Image contrast measurement or images with additional scattered x-rays

Acrylic plates 5 mm thick were stacked to thicknesses of 5–30 mm on a 3 mm diameter plastic fiber in order to evaluate the effect of scattered x rays on image contrast. Image contrasts was obtained as explained in Sec. III B.

D. Spectral analysis of images sharpness

To evaluate image sharpness, spectral analysis of the images was conducted with fast Fourier transformation of the profile data, as shown in the Fig. 4. X-ray images of plant seeds (the diameters of approximately 2 mm) were obtained, and the spectral analysis of the images was also conducted. The plant seeds images were digitized and processed with 2D fast Fourier transformation in order to obtain power spectra of the images.

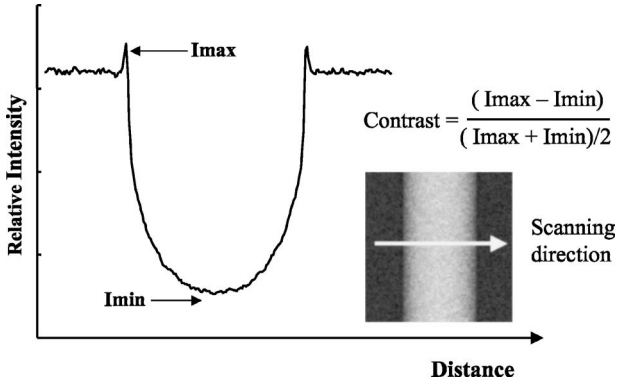

FIG. 5. An example of profile curve of a plastic fiber image. Definition of *I* max and *I* min in contrast for digitized images. The scanning was conducted as the direction of the arrow shown in the plastic fiber image.

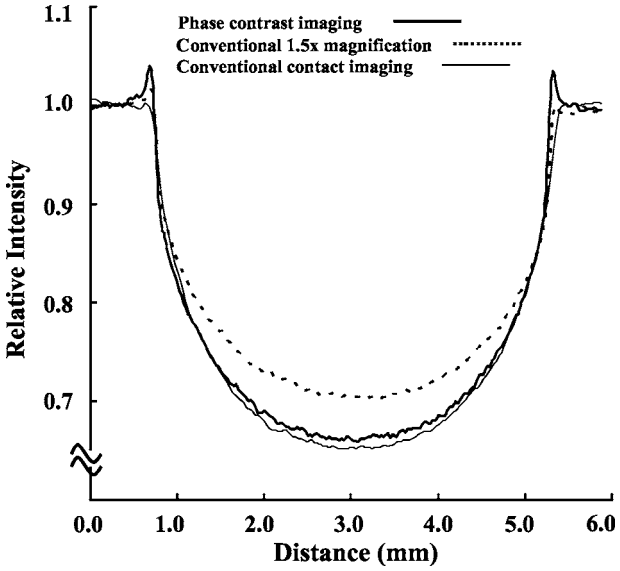

FIG. 6. The contrasts for the phase contrast imaging (solid line), conventional contact imaging (thin line) and conventional 1.5× magnification (dotted line). The sizes of the images were adjusted to be 1.5× magnification for all, for convenience in comparison of intensities at the edges of the fiber images.

IV. RESULTS

A. Evaluation of image contrast due to phase contrast imaging

The x-ray intensity profiles of the 3 mm diameter plastic fiber seen in Fig. 6 compare phase contrast imaging, conventional contact imaging, and conventional 1.5× magnification imaging. In the phase contrast imaging intensity profile, conspicuous edge enhancement was observed, with an increase of image contrast of about 9% (0.448/0.412) over the contact imaging.

B. Effect of scattered x-rays on image contrast

In Fig. 7, it is seen that image contrast decreases with the increase of the thickness of the stacked acrylic plates, which scatter x-rays. With the thickness of the stack of acrylic plates ranging from 0 to 30 mm, conventional contact imaging registered the greatest decrease in image contrast: 44% (0.238/0.428). Conventional 1.5× magnification imaging exhibited an intermediate decrease in image contrast: 30% (0.268/0.382). Phase contrast imaging exhibited the smallest decrease: 22% (0.350/0.448).

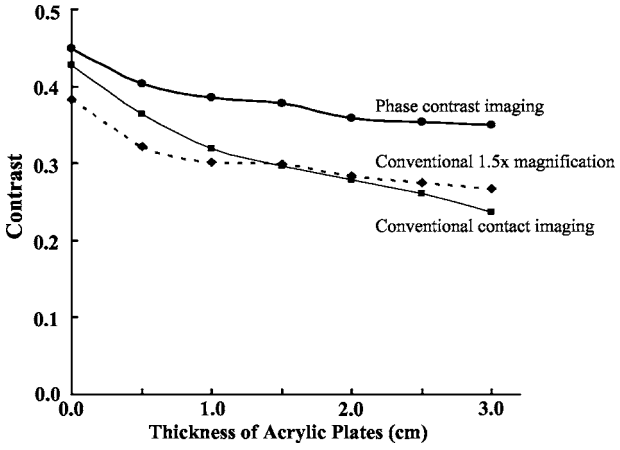

FIG. 7. Comparison of contrasts of the plastic fiber calculated from different thickness of acrylic plates.

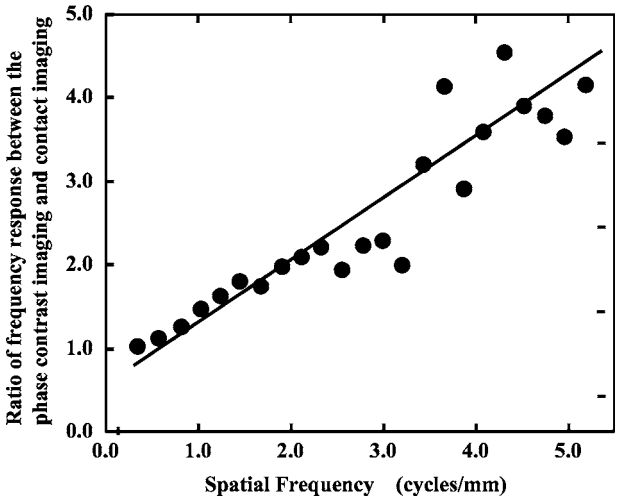

FIG. 8. Ratio of frequency response for the phase contrast imaging over the contact imaging. Note that improvement of sharpness due to phase contrast imaging is more conspicuous in the range of higher spatial frequencies.

The decrease of image contrast caused by the addition of acrylic plates is also due to a hardening effect owing to selective absorption of x-rays by the plates. This hardening effect decreases image contrast equally at each width of stacked plates for the three kinds of imaging: The conventional contact imaging, the conventional 1.5× magnification, and the phase contrast imaging.

C. Spectral analysis of the images

Figure 8 presents ratios of spatial frequency response of the phase contrast imaging of the plastic fiber over that of the conventional contact imaging. The ratios rise steadily to a ratio of approximately 4 at 5.0 cycles/mm, the highest spatial frequency in our analysis. This result suggests that sharpness would be increased more greatly with smaller sized objects.

Figure 9 shows plant seeds images with conventional contact imaging (left) and with phase contrast imaging (right). The power spectra at various spatial frequencies are shown in Fig. 10. The power spectra of the phase contrast imaging are higher than those of the conventional contact imaging in all spatial frequencies in our analysis.

V. DISCUSSIONS

A. Image sharpness

In phase contrast imaging, edge enhancement is caused by the refraction of x-ray flux. When x-rays are coherent laterally, stronger edge enhancement is observed due to the interference of x-ray beams.[4] In the case of x-ray tubes for medi-

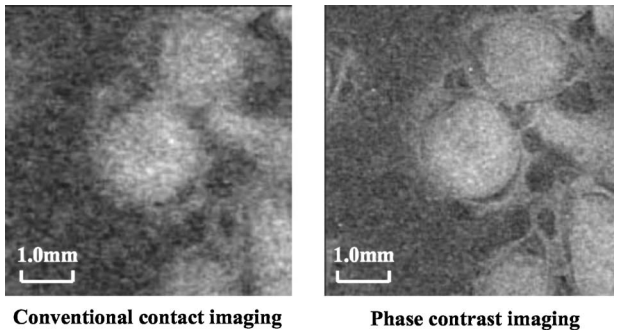

FIG. 9. Digitized images of plant seeds embedded in glue. The left is for the conventional contact imaging, and the right is for the phase contrast imaging.

cal use, the coherence is not great enough for interference because the focal spot size is 0.1 mm or greater and because the distance between the x-ray source and the object is in the range of 0.5–2m.[17] However, edge effect due to the refraction of x-ray flux can be obtained in the conditions which Honda and co-workers have reported,[5] although the edge enhancement is not as strong as that obtained with micro-focus x-ray tubes whose focal spot is small enough for laterally high coherence. In other words, the conditions for the phase contrast imaging using practical x-ray tubes for medical use are a small sized focal spot, such as 0.1 mm, and specific distances between the x-ray source and the object and between the object and an x-ray detector.[15] Since the x-ray detector is positioned away from the object in the phase contrast imaging takes place, and the rescaling effect increases the modulation transfer function (MTF) of the image when geometric blurring is small enough.[18] This increase in MTF improved image sharpness as well as increased image contrast at the fringes of the object in this study, suggesting that phase contrast imaging using practical x-ray tubes for medical use would improve image sharpness and aid diagnoses.

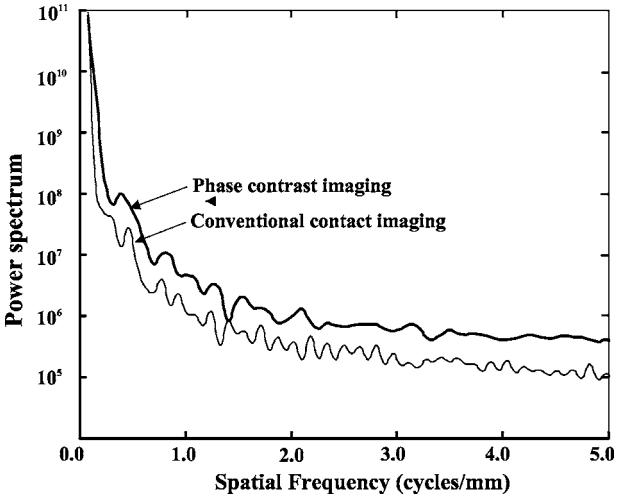

FIG. 10. The power spectra of the images for plant seeds as shown in Fig. 9 for the phase contrast imaging (solid line) and the conventional contrast imaging (thin line).

B. Spectral analysis of image sharpness

It is well-known that edge effect increases image sharpness in the unsharp masking process of digital x-ray images and in the development of silver halide photographic films; this is the so-called "adjacent effect." The method of analyzing image sharpness is well established in dealing with the adjacent effect in film development,[19] and the method has been applied to the simulation of image sharpness obtained via phase contrast imaging by Ohara and co-workers.[7] We have utilized their theoretical approach in our experimentation.[6]

Edge enhancement due to phase contrast imaging takes place at the boundaries between the materials whose refraction indices differ from each other. Consequently the improvement of the sharpness of the image is limited to these areas, while MTF is used to evaluate the entire image. In aid of diagnosis, morphological changes revealed by an x-ray image are important indicators in the detection of abnormalities of the function. Thus in such use of x-ray images, an increase of contrast at fringes of objects is substantially equivalent to an increase in MTF.

C. Scattered x-rays

In mammography, scattered x rays from an object cannot be avoided, and the effect on image contrast is considerable. As noted earlier, in our experimentation with acrylic plates stacked to a thickness of 30 mm, image contrast decreased by 44% with conventional contact imaging without any anti-scatter grid, by 30% with conventional 1.5× magnification, and by 22% with phase contrast imaging, as seen Fig. 7. These varying differences of image contrast loss can be attribute to the varying distances between the object and the screen-film cassette in each of the three methods. The distance between the object and the x-ray detector is greatest with the phase contrast imaging, and this creates an air-gap effect which diminishes x-ray scattering.[6] This air-gap effect in phase contrast imaging helps maintain image contrast, so that phase contrast imaging apparatus can operate without any anti-scattering x-ray grid and yet not sacrifice image quality to scattered x-rays when imaging thick objects or operating at higher tube voltages.[20]

In addition to scattered x-rays, the hardening effect, mentioned earlier, caused by the added acrylic plates decreased image contrast. This effect decreased the contrast values seen in Fig. 7, but it had no comparative effect among the three imaging methods at each thickness of the acrylic plates.

D. Radiographic mottles in our empirical study

The granularity of an image or radiographic mottle affects the measurement of image sharpness. Radiographic mottle consists of quantum mottle, structure mottle, and film graininess. The effects of the latter two are equal in all of our imaging because a single type of screen-film system was used in our experiments; quantum mottle alone accounts for any difference in measured sharpness in our experiments. In

our study, x-ray exposures were adjusted such that optical density of the films was 1.40±0.05 for all imaging. Since film density depends on the flux of x-ray quanta, the quantum noise in all of the images we obtained was approximately the same, although the exposure of the object to x-rays differed depending on geometrical conditions.

E. Detector-resolution and phase contrast

The half width of the edge enhancement, E, for 0.7 Å x-ray (Mo $K\alpha$) is reported by Ishisaka and co-workers to be 49 μm, using their Eq. (1).[15] They have also reported that the half width of the edge enhancement above on blurring of 47 μm is theoretically 96 μm, which falls within the 100±20 μm of their empirical results with a practical molybdenum anode x-ray tube for mammography. In our experiment, our magnification ratio was 1.50, while the results by Ishisaka and co-workers above are based upon a magnification of 1.47. The half width that we obtained for the edge enhancement shown in Fig. 6 comprises four 25 micron pixels, 100 microns in sum. Thus, if the phase contrast image were digitized with pixels as large as 100 micron, the edge enhancement, which would otherwise be observable by naked eyes on the film, would be lost. However, because screen-film mammography has resolution of 20 lines/mm, which corresponds to 25 micron pixels in digital images, the edge effect can be successfully duplicated in the film image by using 25 micron pixels.

F. Medical implications of the phase contrast imaging

In our results, as shown in Fig. 8, the improvement of sharpness is greater at higher spatial frequencies, implying that the detectability of details important in mammographic images would increase. As seen in Fig. 10, a higher power spectrum was observed for an image of plant seeds produced through phase contrast imaging than for a corresponding image produced through conventional contact imaging. This higher power spectrum coincides with improved sharpness of same-sized x-ray images created with digitized data for phase contrast imaging and the conventional contact imaging. Since the diameters of plant seeds we imaged are smaller than that of the plastic fiber we imaged, the difference of the power spectrum for plant seeds at 5 cycles/mm in Fig. 10 is 20% and smaller than the 44% (0.238/0.428) observed in Fig. 7 because of the smaller diameters, r, of the objects. As a result, edge effect is as small as interpreted in Eq. (1). In addition, the value of δ shown in Eq. (1) is smaller for the images of plant seeds surrounded by glue than for those of a plastic fiber surrounded by air, while the edge effect in the image of the plant seeds is weak compared with that in the image of the plastic fiber. The increase of the power spectrum in the range of lower spatial frequencies in Fig. 10 can be ascribed to the magnification effect on noise[21] that spatial frequency shifts higher owing to magnification in the digital data image for phase contrast imaging.[7] The air gap effect would increase the image contrast due to a decrease of scattered x rays that also increases the power spectrum values for phase contrast imaging in the range at all spatial frequency. We may say that both phase contrast and the air gap effect increase the power spectrum for phase contrast, although it is difficult to estimate the relative strength of each effect qualitatively from our experiments here. However, the increase in the range of higher spatial frequency would be due mainly to phase contrast as shown in Fig. 8.

It has been reported that it is difficult to detect tumors surrounded by glandular tissues with screen-film mammography system in contact imaging, especially for dense breast images.[22] The reason given is that the difference in the absorption of x-rays between the tumor and surrounding glandular tissues is too small to create a detectable difference in the optical density of the film. Since the sensitivity in phase contrast is about a thousand times higher than one in absorption contrast,[3] improved detectability of tumors in glandular tissues can be expected from phase contrast mammography. As is shown in Fig. 7, phase contrast imaging would create high-contrast images even with dense breasts. The phase contrast imaging reported here would be expected to be a new method useful for medical imaging when the increase of x-ray exposure on object is avoided with such higher speed screen-film systems as Honda and co-workers have reported[14] or with digital x-ray detectors.[6]

VI. CONCLUSION

We have evaluated and analyzed the image quality in a phase contrast imaging system using customized mammography equipment. Results indicated better image sharpness from phase contrast imaging than from for conventional contact imaging or conventional magnification imaging. In addition, the phase contrast imaging reduces the effect of x-ray scattering because of its air-gap effect. Our study suggests that phase contrast imaging would be highly useful in mammography.

ACKNOWLEDGMENTS

The authors appreciate fruitful discussion with Dr. Chika Honda and Mr. Hiromu Ohara of Konica Minolta Medical and Graphic, Inc. We also thank Professor Kiyoshi Murata of Shiga University of Medical Science and Mr. Kazutaka Masuda of Shiga University of Medical Science Hospital for their permission to publish this work.

APPENDIX: THE OUTLINE ON FORMULATION FOR THE HALF WIDTH OF PHASE CONTRAST

A theoretical consideration of x-ray refraction indicates that the x-ray image receptor must be separated from the object for the phase contrast edge effect to be observed,[1] as shown in Fig. 1. X-ray flux is increased just outside the edge of the cylinder image, and is decreased just inside that image edge, resulting in the edge enhancement or the edge effect as described in the theory.

We have considered phase contrast using refraction theory in order to estimate the edge enhancement quantitatively.[15] A schematic diagram of x-ray refraction for our formulation is shown in Fig. 11. It is assumed that the x-ray source is a point source, and that the cylindrical object does not absorb x

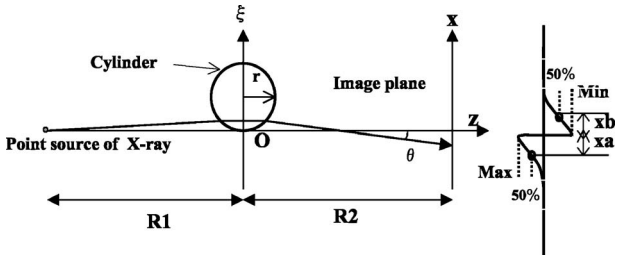

FIG. 11. Schematic diagram of x-ray refraction.

rays. A monochromatic x-ray beam from the point source refracts after passing through the cylindrical object with radius r at a small distance ξ from the z axis, then is incident on the image plane. The position, x, of the intersection of the x ray and the image plane on the x-axis is expressed as

$$x = \xi(1 + R2/R1) - R2 \times \delta(2r)^{1/2}/\xi^{1/2}. \quad \text{(A1)}$$

Note that the x-ray refractive index of solids is expressed as $n=1-\delta-i\beta$, where δ is the phase shift term, i is the square root of -1, and the β is the absorption term.

A relationship between refractive index and light path length after passing through an object approximates to be mathematically equivalent to the relationship between absorption index and light intensity after passing through an object.[2] Therefore, the intensity at the image plane can be expressed approximately as the second differential of the deviation of the light path after passing through an object. Then, the deviation in the x-ray spherical wavefront induced by passing through a boundary between two different refraction indices was formulated. In this manner, we obtained x-ray intensity at the image plane.[15]

When $x \geqq 0$, the x-ray intensity at the image plane, I, is expressed by Eq. (A2), where the intensity of x rays traveling directly from the x-ray source and intersecting the image plane is set to unity and magnification is $M=1+R2/R1$.

$$I = (1 + R2/R1)/\{1 + R2/R1 + R2 \times \delta(2r)^{1/2} \times \xi^{-3/2}/2\}. \quad \text{(A2)}$$

However, when $x<0$, the intensity, I, is expressed by Eq. (A3), which is based on Eq. (A2) but also accounts for the superposition of the x rays traveling directly from the x-ray source with those which have passed through the cylindrical object.

$$I = 1 + (1 + R2/R1)/\{1 + R2/R1 + R2 \times \delta(2r)^{1/2} \times \xi^{-3/2}/2\}. \quad \text{(A3)}$$

Note if $\delta>0$, the object functions as a diverging x-ray lens so that X-rays passing through the object are not superimposed.

The half-width of edge enhancement, E, in Fig. 4 is defined as $E=-xa+xb$. The value of xa $(xa<0)$ is defined as x where $I(x)=(I\max+1)/2$, and xb $(xb>0)$ is defined as x where $I(x)=(I\min+1)/2$. The intensity at $x\to 0$ where $x<0$ is the maximum, Imax, and at $x\to 0$ where $x \geqq 0$ is the minimum, I min. The calculated value of ξ corresponding to $x=0$ is submitted in Eqs. (A2) and (A3). Thus I min is $2/3$ and I max is $5/3$.[5] Note that I min and I max are constants independent of the variables $R1$, $R2$, δ, or r under the extreme preconditions of the x-ray point source and $x\to 0$.

Using the value of I max above, and Eqs. (A1) and (A3), xa is obtained below:

$$xa = -1.2(1 + R2/R1)^{1/3}\{R2\,\delta(2r)^{1/2}\}^{2/3}. \quad \text{(A4)}$$

In the same manner, xb is obtained using the value of I min, Eqs. (A1) and (A2) as:

$$xb = 1.1(1 + R2/R1)^{1/3}\{R2\,\delta(2r)^{1/2}\}^{2/3}. \quad \text{(A5)}$$

Thus, E is written as:

$$E = -xa + xb = 2.3(1 + R2/R1)^{1/3}\{R2\,\delta(2r)^{1/2}\}^{2/3}. \quad \text{(A6)}$$

Equation (A6) and (1) show that the greater the value of $R2$, the greater the value of E. Similarly, for the size of the object, the greater the radius r, the greater the value of E. The value of E also depends on $R1$. The value of δ is usually so small that the effect of phase contrast is not easily observed with contact radiography. It is important, then, to be able to estimate the width of the edge effect obtainable through phase contrast imaging and optimize the imaging parameters (e.g., $R1$ and $R2$) so as to enhance the edge effect.

[a]Electronic mail: matsuo@belle.shiga-med.ac.jp

[1]V. A. Somenkov, A. K. Tkalich, and S. Sh. Shilshtein, "Refraction contrast in X-ray introscopy," Sov. Phys. Tech. Phys. **36**, 1309–1311 (1991).
[2]K. Iwata, "The technical development of X-ray the phase contrast imaging," M&E, March, 112–117(2000) (in Japanese).
[3]A. Momose, "Phase contrast X-ray imaging," Synchrotron Radiat. **10**(3), 23–35 (1997) (in Japanese).
[4]S. W. Wilkins, T. E. Gureyev, D. Gao, A. Pogany, and A. W. Stevens, "Phase contrast imaging using polychromatic hard X-rays," Nature (London), **384**, 335–338 (1996).
[5]H. Ohara, A. Ishisaka, C. Honda, F. Shimada, and T. Endo, "Phase Contrast Mammography Using a Practical Mo Tube," Radiology, **217**(P), 165 (2000).
[6]M. T. Freedman, S. B. Lo, C. Honda, E. Makariou, G. Sisiney, E. Pien, H. Ohara, A. Ishisaka, and F. Shimada, "Phase contrast digital mammography using molybdenum X-ray: Clinical implications in detectability improvement," Proceedings SPIE Conference on physics of medial imaging, Vol. 5030, 533–540 (2003).
[7]H. Ohara, C. Honda, A. Ishisaka, and F. Shimada, "Image quality in digital phase contrast imaging using a tungsten anode X-ray tube with a small focal spot size," Proceedings SPIE Conference on physics of medial imaging, Vol. 4682, 713–723 (2002).
[8]R. Fizgeral, "Phase-sensitive X-ray imaging," Phys. Today, July 23–26 (2000).
[9]E. Burattini, E. Cossu, C. Di Magio, M. Gambacci, P. L. Indovina, M. Marziani, M. Pocek, S. Simeoni, and G. Simonetti, "Mammography with synchrotron radiation," Radiology, **195**, 239–243 (1995).
[10]T. Takeda, A. Momose, K. Hirano, S. Haraoka, T. Watanabe, and Y. Itai, "Human carcinoma: Early experience with phase-contrast X-ray CT with synchrotron radiation? comparative specimen study with optical microscopy," Radiology, **214**, 298–301 (2000).
[11]N. Yagi, Y. Suzuki, K. Umetani, Y. Kohmura, and K. Yamasaki,"Refraction-enhanced X-ray imaging of mouse lung using synchrotron radiation source," Med. Phys., **26**(10), 2190–2193 (1999).
[12]D. Gao, A. Pogany, A. W. Stevenson, T. Gureyev, and S. W. Wilkins, "X-ray phase contrast imaging study of soft-tissue and bone samples," Proc. SPIE Conference on Physics of Medical Imaging, 3659, 346–355 (1999).
[13]D. Gao, A. Pogany, A. W. Stevenson, and S. W. Wilkins, "Phase-contrast radiography," Imaging Therapeutic Tech. **18**, 1257–1267 (1998).

[14]C. Honda, H. Ohara, A. Ishisaka, F. Shimada, and T. Endo, "X-Ray the phase contrast imaging using small focus X-ray tubes," Japanese J. Medical Physics, **22**(1), 21–29 (2002) (in Japanese).
[15]A. Ishisaka, M. Ohara, and C. Honda, "A new method of analys is edge effect in phase contrast imaging with incoherent X-ray," Opt. Rev., **7**(6), 566–572 (2000).
[16]T. E. Guereyev, A. E. Stevenson, D. Paganin, S. C. Mayo, D. Gao, and S. W. Wilkins, "Quantitative methods in phase-contrast X-ray imaging," J. Digit Imaging, **13**(2), Suppl 1(May), 121–126 (2000).
[17]X. Wu, and H. Liu, "Clinical implication of x-ray phase contrast imaging: Theoretical foundations and design considerations," Med. Phys., **30**(8), 2169–2179 (2003).
[18]C. C. Show, X. Liu, M. Lemacks, J. X. Rong, and G. J. Whitman, "Optimization of MTF and DQE in magnification radiography? a theoretical analysis," Proceedings SPIE Conference on physics of medial imaging, 3977, 466–472 (2000).
[19]M. A. Kriss, "Image Structure," in *The Theory of the Photographic Process*, 4th ed. edited by T. H. James (Macmillan Publishing, New York, 1977), pp. 609–613.
[20]E. F. Donnelly and R. R. Price, "Quantification of the effect of kVp of edge—enhancement index in phase-contrast radiography," Med. Phys. (6), 999–1002 (2002).
[21]K. Doi and H. Imhof, "Noise reduction by radiographic magnification," Radiology, **122**, 479–487 (1977).
[22]S. Hasegawa, K. Oonuki, J. Nagakubo, A. Kitami, K. Ooyama, R. Koizumi, and N. Ouchi, "Breast cancer imaging by mammography: Effects of age and breast composition," J. Jpn. Assoc. Breast Cancer Screen, **12**(1), 101–107 (2003) (in Japanse).